Preparation and Characterization of Electrospun Polyurethane–Polypyrrole Nanofibers and Films

Meltem Yanilmaz,[1] Fatma Kalaoglu,[1] Hale Karakas,[1] A. Sezai Sarac[2]

[1]*Textile Engineering Department, Istanbul Technical University, Turkey*
[2]*Chemistry Department, Polymer Science & Technology, Istanbul Technical University, Turkey*

Received 25 January 2011; accepted 26 February 2011
DOI 10.1002/app.36386
Published online in Wiley Online Library (wileyonlinelibrary.com).

ABSTRACT: Polyurethane (PU)–polypyrrole (PPy) composite films and nanofibers were successfully prepared for the purpose of combining the properties of PU and PPy. Pyrrole (Py) monomer was polymerized and dispersed uniformly throughout the PU matrix by means of oxidative polymerization with cerium(IV) [ceric ammonium nitrate Ce(IV)] in dimethylformamide. Films and nanofibers were prepared with this solution. The effects of the PPy content on the thermal, mechanical, dielectric, and morphological properties of the composites were investigated with differential scanning calorimetry (DSC), dynamic mechanical analysis (DMA), Fourier transform infrared (FTIR)–attenuated total reflection (ATR) spectroscopy, dielectric spectrometry, and scanning electron microscopy. The Young's modulus and glass-transition temperatures of the composites exhibited an increasing trend with increases in the initially added amount of Py. The electrical conductivities of the composite films and nanofibers increased. The crystallinity of the composites were followed with DSC, the mechanical properties were followed with DMA, and the spectroscopic results were followed with FTIR–ATR spectroscopy. In the composite films, a new absorption band located at about 1650 cm^{-1} appeared, and its intensity improved with the addition of Py. The studied composites show potential for promising applications in advanced electronic devices. © 2012 Wiley Periodicals, Inc. J Appl Polym Sci 000: 000–000, 2012

Key words: conducting polymers; nanofibers; polyurethanes

INTRODUCTION

The rapid development of electronic technology has brought about a demand for materials with good physical and mechanical properties. Composite materials are defined as a multicomponent materials comprising multiple different phase domains in which at least one type of phase domain is a continuous phase. Recently, composite materials have drawn extensive attention from scientists all over the world because of their interesting mechanical, electrical and thermal properties and, potential applications.[1,2] Polyurethanes (PUs) are segmented polymers built up from soft and hard segments. They have a highly elastomeric behavior, abrasion and chemical resistance, clarity, and tensile strength.[3,4]

Electrically conductive polymers have become very popular in the past years because of the fact that they have the physical and chemical properties of organic polymers and good electrical characteristics. Polypyrrole (PPy) is one of the most widely studied conductive polymers because of the aqueous solubility of the monomer and its low oxidation potential, easy synthesis, long-term ambient stability, redox properties, and high conductivity.[5–7] Antistatic applications, electromagnetic shielding, filters, dust- and germ-free clothing, camouflage and stealth technology, actuators, and polymer batteries are among the practical applications of PPy. However, its inherently poor solubility in common solvents, which originates from strong interchain and intrachain interactions, has limited the practical applications of PPy.[8–10] Wen et al.[11] described the effect of conducting PPy on the morphology and ionic conductivity of thermoplastic PU impregnated with oxidant and pyrrole (Py), which was doped with $LiClO_4$.

Electrospinning is a simple and versatile technique that produces continuous microdiameter and nanodiameter polymer fibers through the action of an external electric field imposed on a polymer solution or on its melted form.[12–17] On the nanometer scale, it is possible that certain properties will be significantly different from those in the bulk, and thus, it is important to characterize nanofibers. Some of the typically superior properties of nanofibers are their high specific surface area, high porosity, small fiber diameter, potential to incorporate active chemistry, filtration properties, low layer thickness, high permeability and low basis weight, high degree of structural perfection, and mechanical properties.[18–22]

Correspondence to: A. S. Sarac (sarac@itu.edu.tr).

There is growing interest in the design and preparation of novel composite nanofibers with improved properties, such as conductivity, filtration capability, antimicrobial characteristics, and waterproofing.[23] To date, numerous studies on the electrospinning of PUs and other polymers have been published.[23–29] PU nanofiber mats exhibit good mechanical properties, so they can be used in the applications from protective textiles to reinforced composites, high-performance air filters, wound dressing materials, sensors, and so on.[25,26] Earlier studies on the electrospinning process of PU focused on the basic principles and processing parameters.[24,28] Recently, several authors have investigated the mechanical properties of electrospun fiber mats.[29,30] Moreover, Zhuo et al.[12] spun nanofibers having shape-memory effects from shape-memory PU solutions by the electrospinning method. In the literature, some studies on the effects of electrospinning on the chain conformations of polymers have been reported, and these have indicated changes in the chain conformations and rapid phase separations that occur because of electrospinning.[15,20,21] Chronakis et al.[5] prepared electrospun nanofibers from a solution mixture of PPy and poly ethylene oxide (PEO); PEO acted as a carrier to improve PPy processability. Also, PPy–Ag nanofiber composites have been synthesized by the redox reaction between silver nitrate and Py monomer.[31] Huang et al.[6] prepared PPy nanofibers in the presence of a functionalized dopant.

The main objective of this work was to study the effects of the PPy content on the PU matrix. Ce(IV) was used to polymerize Py in the PU matrix and to obtain homogeneous composite solutions. The results show that the uniform dispersion of PPy was achieved because of the high oxidation potential of Ce(IV). The effects of PPy on the dielectric, electrical, mechanical, and thermal properties of the composite films and nanofibers are reported in this article. The experimental results indicate that the prepared PU–PPy composites could be a potential material for electronic devices.

EXPERIMENTAL

Materials

Thermoplastic PU was supplied from Flokser Co., Istanbul, Turkey. It was the ester product of polyester polyol and diphenylmethanediisocyanate; the chain extender was 1,4-butanediol. The molecular weight of the PU (93,000 g/mol) was determined by gel permeation chromatography. The solid content of PU was in a 35 wt % solution in dimethylformamide (DMF). Py (C_4H_5N; Sigma-Aldrich, Co., Ltd. Taufkirchen, Germany, analytical), DMF [$(CH_3)_2NC(O)H$; Riedel-de Haen, Seelze, Germany, analytical], ceric ammonium nitrate, CAN, {$(NH_4)_2[Ce(NO_3)_6]$; BDH Reagents and Chemicals, England, analytical}, acetonitrile (Sigma-Aldrich, Co., Ltd. Taufkirchen, Germany, analytical), tetrahydrofuran (Sigma-Aldrich, Co., Ltd. Taufkirchen, Germany, analytical), methanol (technical), and ethanol (technical) were used.

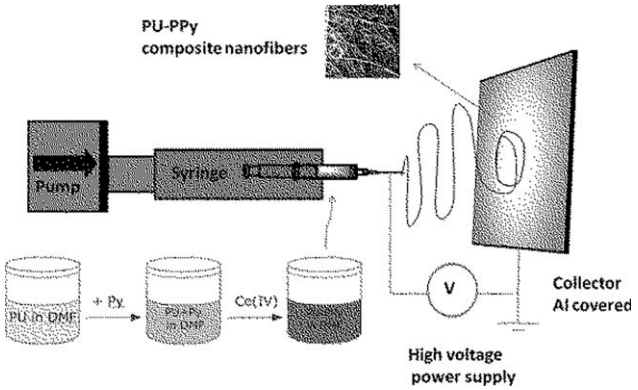

Figure 1 Schematic illustration of the composite nanofiber preparation process.

Preparation of the composite films

PU–PPy composite solutions were prepared by the oxidative polymerization of Py in PU matrix with three components, PU, Py, and Ce(IV). PU was dissolved in DMF, and Py was added to this solution. Ce(IV) was used to oxidize Py on the matrix. Excess solvent was evaporated by the application of heat, and the reaction mixture was cast as a film. The cast solutions were dried in a vacuum oven for 24 h at 80°C. The weight percentages of Py {Py/[Py + PU + Ce(IV)] = 5, 23, 36, 45, and 50%} were calculated and reported with the initial weights of the three components mentioned previously.

Preparation of the composite nanofibers

To prepare the electrospinning solutions (Fig. 1), 2 g of PU was dissolved in a DMF and tetrahydrofuran mixture (1/1 v/v). A controlled amount of Py monomer was added to the solution. Composite solutions with different ratios of Py monomers were prepared at 20% (w/v) in the solvent mixture. Then, Ce(IV) was added to this solution. The electrospinning apparatus consisted of a syringe pump, a high-voltage direct-current (dc) power supplier generating a positive dc voltage up to 30 kV, and a grounded collector that was covered with aluminum foil. The solution was loaded into a syringe, and a positive electrode was clipped onto the syringe needle, which had an outer diameter of 0.8 mm. The feeding rate of the polymer solution was controlled by a syringe pump, and the solutions were electrospun onto the collector. The syringe pump was set at a volume flow rate of 2 mL/h, the applied

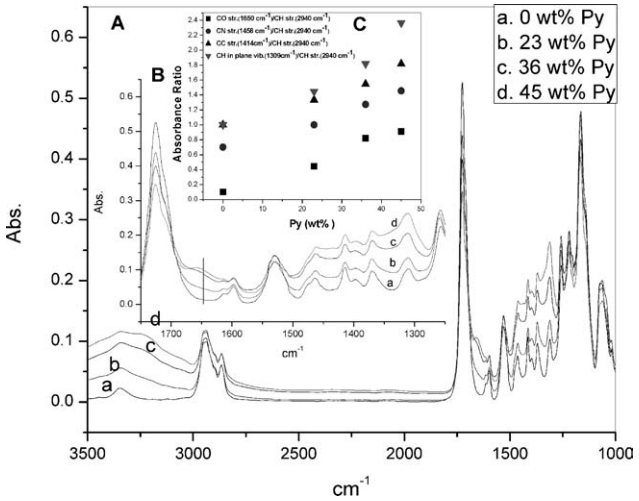

Figure 2 (A) FTIR–ATR spectra of the PU and PU–PPy composite films, (B) spectra between 1750 and 1250 cm^{-1}, and (C) absorbance ratios versus Py concentration.

voltage was 15 kV, the tip-to-collector distance was 10 cm, and all solution preparations and electrospinning were carried out at room temperature.

Characterization of the PU–PPy composite nanofibers

The characteristic functional groups of the samples were analyzed with Fourier transform infrared (FTIR) spectroscopy in the attenuated total reflection (ATR) mode (PerkinElmer FTIR–ATR Spectrum One with a universal ATR attachment with a diamond and a ZnSe crystal, Shelton, USA). The thermal analysis of the PU and PU–PPy composites was performed by differential scanning calorimetry (DSC; TA Instruments, New Castle, DE) at a heating rate of 10°C/min. A TA Q800 model dynamic mechanical analyzer was used to analyze the mechanical properties of the composite film and nanofibers. The alternating-current (ac) measurements were performed with a Novocontrol broadband dielectric spectrometer (Novocontrol Alpha-A high-performance frequency analyzer, frequency domain ¼ 0.001 Hz to 3 GHz, Germany). A Nanoeye SNE 3000M model mini scanning electron microscope (SEC Co Ltd, Suwon Gyunggi-do, Korea) was used to take nanofiber images.

RESULTS AND DISCUSSION

FTIR–ATR spectrophotometric analysis

The structural characterization of the composites was performed with FTIR–ATR spectroscopy. Figure 2 shows the FTIR–ATR spectra of the PU–PPy films and pure PU films. The band centered around 1725 cm^{-1} was attributed to the stretching of free urethane carbonyl groups.[32,33] Hydrogen bonding, one of the most common interactions, was detected by the observation of newly created functional groups and frequency shifts by FTIR spectroscopy.[34] In the composite films, a new broad band located at about 1650 cm^{-1} appeared, and its intensity improved with the addition of Py [Fig. 2(B)]. This new band was assigned to the formation of hydrogen bonding and interactions between the amide carbonyl and NH groups of Py and Ce(III) (Fig. 3), as has been reported in earlier studies.[35,36] These results may explain why the PU–PPy composites had higher glass-transition temperature (T_g) and melting temperature (T_m) values than pure PU, as discussed later.

Moreover, Figure 2(C) shows the linear relationships between the absorbance ratios of certain

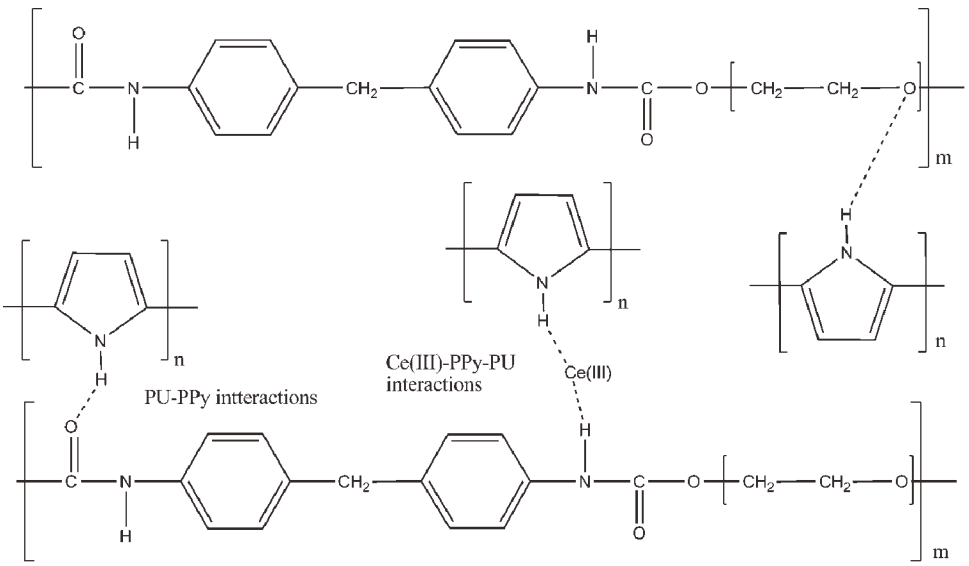

Figure 3 Schematic illustrations of the interactions in the composites.

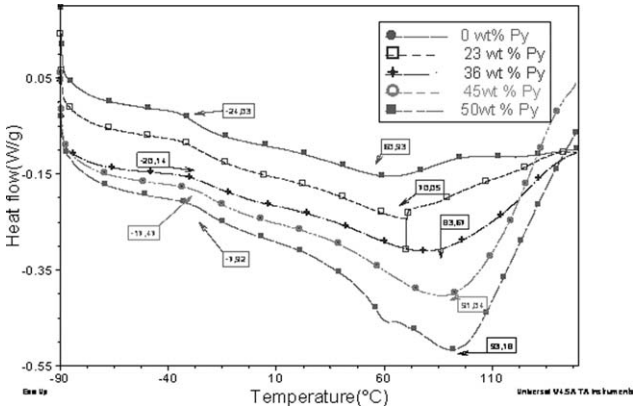

Figure 4 DSC results of the PU and PU–PPy composites.

functional groups corresponding to conjugated polymeric units and Py concentrations. It can be seen from the figure that the absorbances of C=N stretching ($\sim$ 1458 cm^{-1}), C—C stretching ($\sim$ 1414 cm^{-1}), and C—H vibrations ($\sim$ 1309 cm^{-1})[37–39] increased as the concentration of PPy increased.

DSC analysis

In earlier studies, it was found that PU's thermal stability increased with increasing urethane groups because these groups formed urethane–urethane crystalline structures, which had a higher stability than their amorphous counterparts.[40] Also, it was reported[41] that T_g depended on the hard-segment content for different PUs. A higher hard-segment content led to an increase in T_g. The DSC curves for the PU–PPy composite films are presented in Figure 4. The T_g value of PU appeared at -24°C, and the T_g values of the PU–PPy composites appeared between about -20 and -7°C. In general, T_g of PU increased with increasing PPy content in the composites; this suggested that the interaction between PPy and PU occurred through hydrogen bonds formed among the carbonyl groups of PU and amide groups of PPy. This helped to improve their phase mixing.

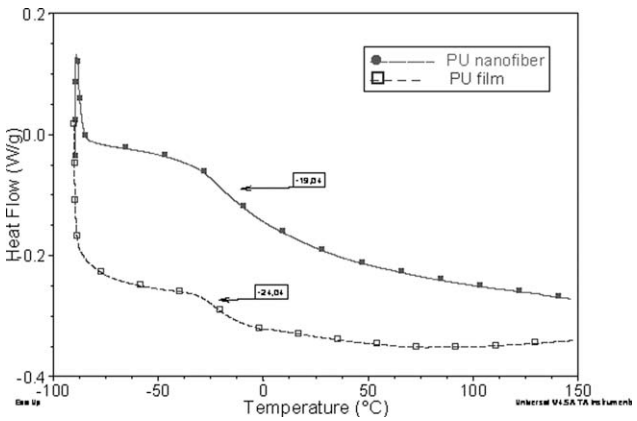

Figure 5 DSC results of the PU film and nanofiber.

Figure 4 also shows that an increase in the Py amount led to increases in the T_m and enthalpy values of the composites. We assumed that the introduction of PPy enhanced the phase mixing, hydrogen bonding, and intermolecular packing of domains in the soft segments. The melting enthalpy and T_m at about 70°C increased with increasing PPy content, and the peak position shifted to higher temperatures (93°C). Also, a new exothermic peak was observed at about 60°C in the presence of a high amount of Py. This was another indication of the interactions and hydrogen bonding among PU, PPy, and Ce(III).

Figure 5 shows the DSC curves of the PU nanofibers and bulk films. It was found that there were differences between the samples, films, and nanofibers, although they had the same composition. It was apparent that higher T_g values were formed in the nanofiber structure. Zhuo et al.[12,13] reported that the crystallization degree in the nanofibers was much higher than that in the bulk form, and the microphase separation in the nanofibers was insufficient in comparison with the bulk PU film. This study supported the idea that electrospinning increases the crystallinity of structure.

In addition to dynamic mechanical analysis (DMA) and DSC analysis, thermogravimetric studies were also used to obtain a better understanding of the developed composites. Thermogravimetric analysis (TGA) and differential thermogravimetry (DTG) curves of PU and PU–PPy composites are shown in Figure 6. Both samples lost less than 3% of their weight below 300°C. Although the PU–PPy composites began to degrade at a temperature about 10°C lower than the pure PU (Fig. 6 inset), that difference was not significant, and the thermostability of the composites was still preserved up to 250°C. The

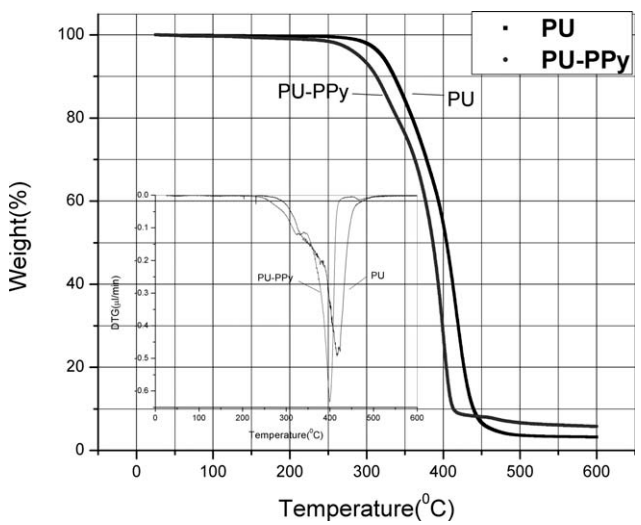

Figure 6 TGA and DTG curves of the PU and PU–PPy composites.

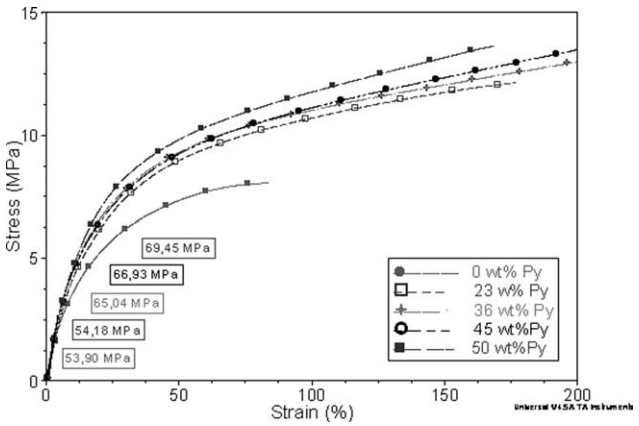

Figure 7 Stress–strain curves.

TGA curve shows that at 400°C, the weight losses were 72.1 and 45.5% for PU–PPy and PU, respectively. Pure PU and the PU–PPy composites had one peak in the DTG curve. However, a small peak between 300 and 350°C was observed in the composite sample. The decomposition of the PU–PPy composite followed a similar tendency as that of the pure PU films. In effect, there was no significant difference between the two TGA thermograms shown in Figure 6. These results were comparable with the findings of Wen et al.[11]

DMA

In general, the hard-segment content has a significant influence on the mechanical and thermomechanical properties of PUs, such as the tensile modulus, maximum stress, and elongation at break. From earlier studies,[41] it is known that interchain crosslinking improves the thermal stability. The modulus increases with crosslinked hard-segment content; this is due to the stiffness of the polymer chain and results from polymeric interactions. The tensile strength of the films is affected by factors such as soft and hard segments in the PU structure, their cohesion energy, degree of packing of the macromolecules, phase separation, and crosslinking degree of PU.[41] Furthermore, the mechanical properties of thermoplastic elastomers depend on the size, shape, and concentration of the crystals in the hard segments. In other words, the ability to crystallize and the amount in the crystalline areas in soft segments also affect the mechanical behavior.[42] More soft segments lead to lower tensile strength, elongation at break, and hardness.[43] The mechanical test results showed that after the addition of PPy, the modulus increased (Fig. 7). Increasing the PPy content changed the properties of the composite films from elastomeric to plasticlike and finally to brittle. So, when the PPy content was increased, the composite became much stronger because of formation of additional hydrogen bonds. This led to enhanced mechanical properties in the composites.

Figure 8 summarizes the DSC and DMA results. We observed that the T_m, T_g, and Young's modulus values increased as a function of the Py content.

ac conductivity and dielectric properties

The electrical conductivities of the composite films are presented in Figure 9(A). Electrical conductivity measurements were carried out at room temperature (25°C). The samples displayed classical dielectric material behavior, with electrical conductivity increasing with frequency for high values of frequency. For the composites, the same type of behavior was observed with higher conductivity levels than in the PU matrix. Figure 9(C) shows the conductivities at 10^7 Hz. There was a correlation between the conductivities and Py contents. In the range 10^3–10^5 Hz, no changes were observed; only at

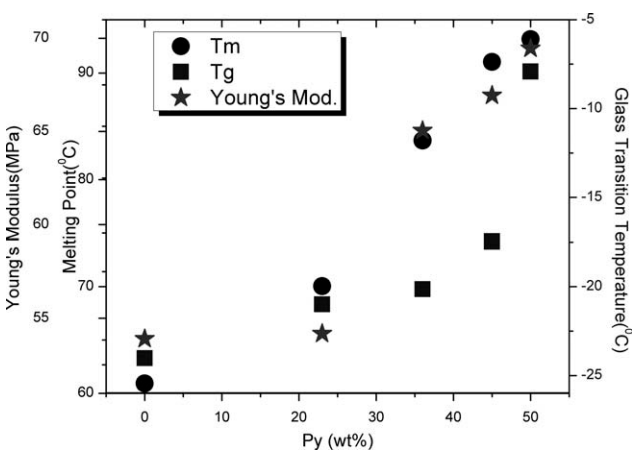

Figure 8 Correlation between the thermal and mechanical properties of the composites and Py content.

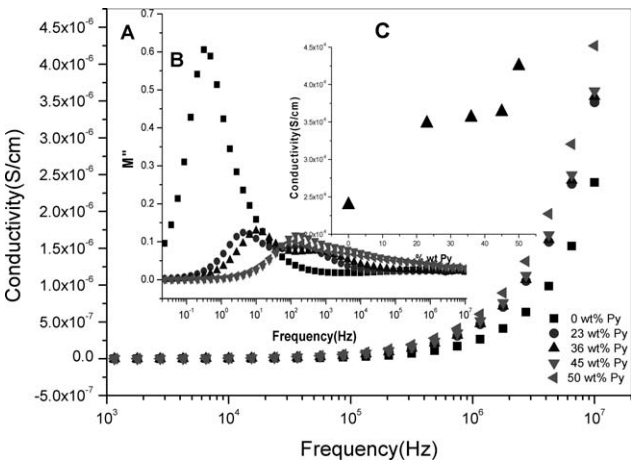

Figure 9 (A) ac conductivity, (B) M'' values versus frequency, and (C) ac conductivity at 10 KHz for the PU–PPy composites.

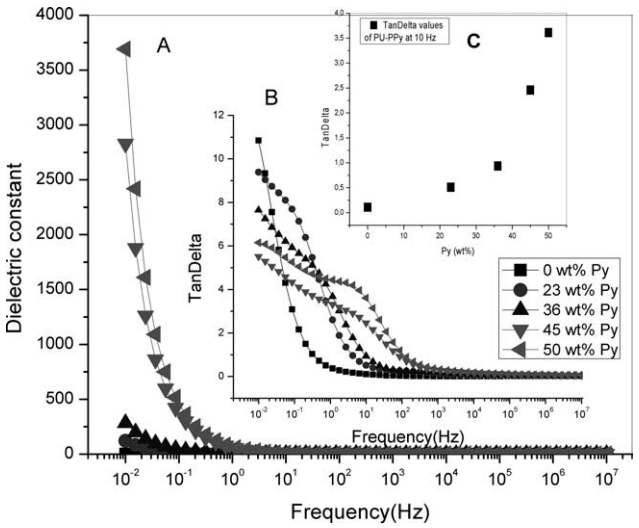

Figure 10 (A) Dielectric constant, (B) tan δ frequency dependence, and (C) tan δ values at 10 Hz for the PU films with different Py contents.

high frequencies we observed a high conductivity with increasing Py content. The conductivity increase with frequency was a polymeric semiconductor behavior and was due to the mobility increase of the charge carriers in the composites. The total frequency-dependent conductivity [σ(ω)] at a given temperature and frequency can be described as follows:

$$\sigma(\omega) = \sigma_{dc} + A\omega^s$$

where σ_{dc} is the direct-current conductivity, A is a constant depending on the temperature, s is the frequency exponent, and $A\omega^s$ shows the ac conductivity.[44] As shown in Figure 9, in the range of 10^3–10^5 Hz, a plateau was observed, which resulted in the conductivity being independent of the frequency. The figure shows that at high frequencies (10^7 Hz), the electrical conductivities of the composite films increased when the quantity of PPy was increased. In the range of 10^5–10^7 Hz, the conductivity increased with the frequency. The increase of ac conductivity at higher frequencies originated from the charge motion in the amorphous region and indicated the presence of isolated polarons in this region.[45,46] As a result, the addition of PPy resulted in an improvement in the conductivity of the composite. Figure 9(B) shows the imaginary part of the electric modulus (M'') for the composites. In the 10^{-1}–10^4 Hz frequency region, we observed a peak for each sample. The frequency position of this peak was proportional to the dc conductivities of the sample, so we concluded that there was an increase in the conductivity of the composites with increasing Py content.

The dielectric constant shows the ability of a material to store electric potential energy under the influence of an alternative electric field.[47] In Figure 10, the effects of the initially added Py content on the dielectric constant at frequencies between 10^{-2} and 10^7 Hz are shown. Compared with neat PU, the addition of PPy caused an increase in the dielectric constant at lower frequencies (10^{-2} to 1 Hz). At 10^{-2} Hz, the dielectric constant increase of the composite films was more obvious when the quantity of Py was increased (for neat PU, the dielectric constant was about 0, and for the composites containing 50 wt % initially added Py, it was about 3750).

The dielectric constant of PU was observed to be independent of frequency throughout the scan range (10^{-2} to 10^7 Hz), whereas the frequency dependency of the dielectric constant increased with the addition of Py above 36 wt % Py. There was an increase in the dielectric constant with the weight percentage of Py at 10^{-2} Hz, because the dielectric constant of PPy was much larger than that of PU. PPy had a higher polarization compared to the pure PU matrix under an electric field. A significant reduction of the dielectric constant was observed with increasing frequency for the range between 10^{-2} and 1 Hz for all of the PU–PPy composites, especially composites with higher PPy, because interfacial electric dipoles had insufficient time periods to follow the variation of the electric field direction at high frequency. The dielectric constant of the polymers decreased gradually with increasing frequency because the response of the electronic, atomic, and dipolar polarizable units varied with frequency. At low frequencies and high concentrations, the dipole movements and charge carriers freely moved within the material under testing and followed the variation of the electromagnetic field, whereas at higher frequencies, the dipole and charge carriers became unable to follow the variations of the applied electric field. This resulted in a decrease in the dielectric constant.[48] We also observed similar results for our samples, as shown in Figure 11.

The dissipation factor or loss tangent is the ratio of the loss factor to relative permittivity. It is a measure of the ratio of the electric energy loss to the energy stored in an applied cyclic electric field. The plot of the tan δ values of pure PU and the PU–PPy composites as a function of the applied frequency is shown in Figure 10(B). It is apparent in Figure 10(C) that composites with a greater amount of PPy in the matrix had higher tan δ values at 10 Hz. The significant enhancement in the dissipation factor contributed to the improvement in the electromagnetic interference (EMI) shielding efficiency.[47] As a result, the PU–PPy composites may prove to be an ideal material for use in EMI shielding applications.

The ac conductivity measurements of the PU–PPy nanofibers were carried out at room temperature. The conductivities of the pure PU nanofibers and PU–PPy

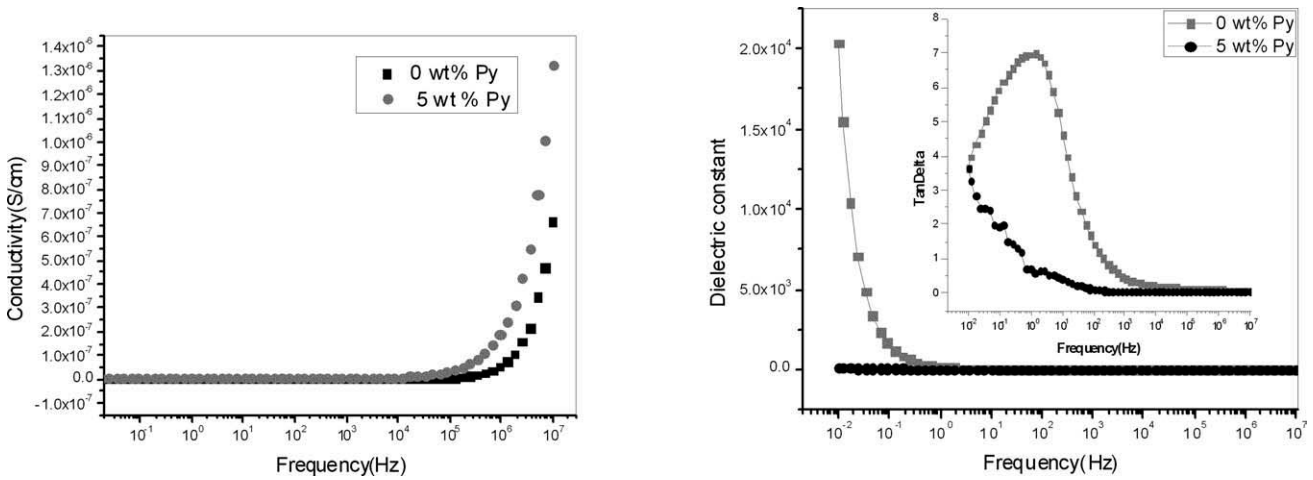

Figure 11 ac conductivities, dielectric constants, and tan δ values for PU and the PU–PPy nanofibers.

composite nanofibers are presented in Figure 11. The ac conductivities of the PU nanofibers without Py and with 5% Py were found to be about 7×10^{-7} and 1.4×10^{-6} S/cm, respectively, at 10^7 Hz.

The changes in tan δ (= ε″ the out-of-phase component or loss modulus/ε′ in-phase component or storage modulus) according to frequency for the pure PU nanofibers and PU–PPy composite

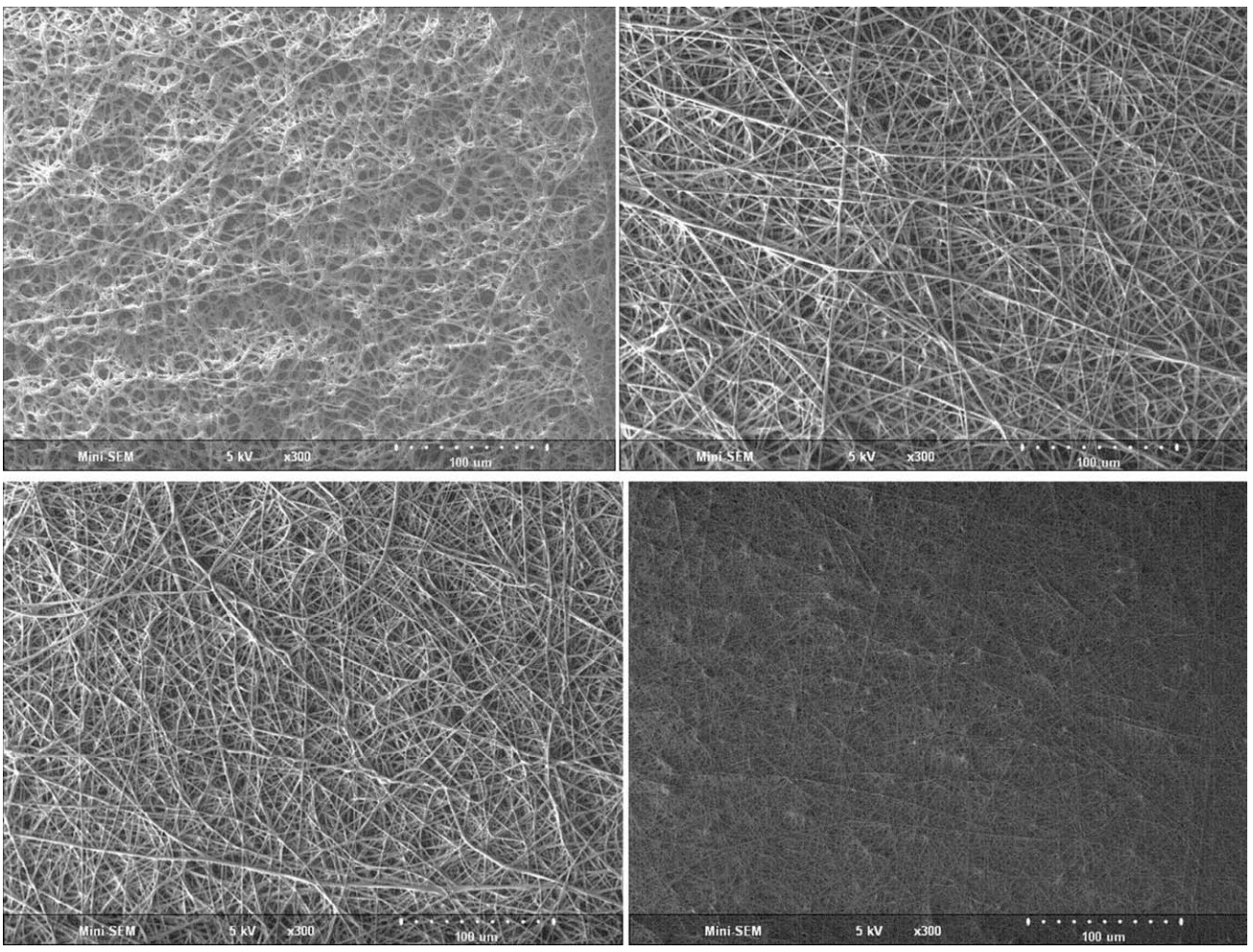

Figure 12 Different morphologies of the PU nanofibers with different Py contents: PU nanofibers, PU–PPy nanofibers (5% Py), PU–PPy nanofibers (7.5% Py), and PU–PPy nanofibers (12.5% Py).

nanofibers is shown in Figure 11 (right graph). The composites exhibited a high dielectric constant and tan δ values in the low- and radio-frequency ranges, so they could be used in charge-storing devices, decoupling capacitors, and EMI shielding applications.[49] In our study, the high values of tan δ make the PU–PPy nanofibers suitable for these applications.

Morphology of the nanofibers

Figure 12 shows the scanning electron micrographs of the PU and PU–PPy composite nanofibers. These morphologies could be attributed to the lower evaporation rate of the electrospinning solvents. Interestingly, the average fiber diameters decreased with increasing PPy content. The average diameter of the PU fibers were about 2 μm, and the diameter of the PU–PPy composite fibers decreased with increasing Py content (∼ 1.6 μm for 5% Py and ∼ 1.3 μm for 7.5% Py). Charge carriers such as salts or conductive components have an influence on the conductivity of the solution. It was found[3,20] that the addition of polyelectrolyte increased the charge density of poly (ethylene oxide) solution, and thus, stronger elongation forces were imposed to the jets because of the self-repulsion of the excess charges under the electrical field. This yielded electrospun nanofibers with a substantially straighter shape and smaller diameter. In this study, the decrease of the average fiber diameters may have been mainly due to the increased charge density of the PU–PPy solutions. As the electrical conductivity of the solutions containing PPy increased, the electrospun fiber diameter decreased. It was observed from the scanning electron images that uniform composite nanofibers were obtained. However, after the limit percentage of Py (12.5% Py for this work), some beads and loops were observed. The effects of fillers and additives on the fiber diameter varies depending on the polymer, system, solvents, and additives.[16] It should be noted that the second component of systems may interact with the solvents, polymers, or both. The electrospinnability of the solution may change as a result of these interactions. Because of strong interaction between PU and PPy, the spinnability of the composite solution was very sensitive to the amount of Py. The optimization of process parameters was very essential for this system because of the electroactive character of PPy and the interactions of the components. Irregularities, such as the so-called beads-on-a-string morphology, began to appear with increasing PPy content, and this was most likely due to the increasing solution conductivity and viscosity induced by the PPy phase. Ji et al.[50] prepared carbon nanofibers through the electrospinning of a blend solution of polyacrylonitrile and PPy and found a similar trend in nanofiber diameter.

CONCLUSIONS

In this work, PU–PPy composite films and nanofibers were successfully prepared for the purpose of combining the properties of PU and PPy. Furthermore, the role of PPy in the electrical, thermal, chemical, and mechanical properties of the composites and the morphological properties of the composite nanofibers was analyzed. The increase in PPy resulted in increased conductivity. The Young's modulus and T_g values of the composites increased with increasing PPy loading. PPy behaved like hard segment in the PU matrix. The hard segment restricted the mobility of the soft segment because of the increased crystallinity of the hard segment with greater Py concentration. The DSC curves confirmed that an increased Py amount in the composites was favorable for crystallization of the hard segment. The composites showed uniform nanofiber morphology, and the FTIR–ATR and DSC results confirmed the compound interactions among the PPy, reduced form of oxidant, and PU. The PU composites in the form of nanofibers and films containing PPy may find promising applications in dielectrics for advanced electronic devices.

References

1. Sui, G.; Jana, S.; Zhong, W. H.; Fuqua, M. A.; Ulven, C. A. Acta Mater 2008, 56, 2381.
2. Kumar, S.; Rath, T.; Mahaling, R. N.; Reddy, C. S. Mater Sci Eng B 2007, 141, 61.
3. Jeong, E. H.; Yang, J.; Young, J. H. Mater Lett 2007, 61, 3991.
4. Lee, K. Macromol Res 2005, 13, 5, 441.
5. Chronakis, I. S.; Grapenson S.; Jakob, A. Polymer 2006, 47.
6. Huang, K.; Wan, M.; Long, Y.; Chen Z.; Wei, Y. Synth Met 2005, 155, 495.
7. Rajagopalan, R. J.; Iroh, O. Appl Surf Sci 2003, 218, 58.
8. Oh, K. W.; Hong, K. W. Text Res J 2001, 71, 726.
9. Brady, S.; Diamond, D.; Lau, K. Sens Actuators A 2005, 119, 398.
10. Wang, Y.; Sotzing, G. A.; Weiss, R. A. Chem Mater 2005, 20, 2574.
11. Wen, T.; Hung, S.; Digar, M. Synth Met 2001, 118, 11.
12. Zhuo, H.; Hu, J.; Chen, S. Polymer 2008, 62, 2074.
13. Zhuo, H.; Hu, J.; Chen, S.; Yeung, L. J Appl Polym Sci 2008, 109, 406.
14. Bhardwaj, N.; Kundu, S. C. Biotechnol Adv 2010, 28, 3, 325.
15. Stephens, J. S.; Chase, D. B.; Rabolt, J. F. Macromolecules 2003, 37, 877.
16. Heikkila, P.; Harlin, A. Express Polym Lett 2009, 11, 437.
17. Yen, F. S.; Hong, J. Polymer 1997, 30, 7927.
18. Wang, H.; Ding, J.; Lee, B.; Wang, X.;Lin T. J Membr Sci 2007, 303, 119.
19. Deitzel, J. M.; Kleinmeyer, J.; Harris, D. Polymer 2000, 42, 261.
20. Park, J. Y.; Han, S. W.; Lee, I. H. Ind Eng Chem 2007, 13, 1002.
21. Rutledge, G. C.; Fridrikh, S. V. Adv Drug Delivery Rev 2007, 59, 1384.
22. Qian, Y. F.; Su, Y.; Li, X.; Wang, H. S.; He, H. C. Iranian Polym J 2010, 19, 123.

23. Tang, C.; Chen, P.; Liu, H. Polym Eng Sci 2008, 48, 1296.
24. Kimmer, D. Nano Con 2009, Rožnov pod Radhoštěm, Czech Republic 2009, 88.
25. Jeon, H. J.; Kim, J. S.; Kim, T. G.; Kim, J. G.; Yu, W. R.; Youk, J. H. Appl Surf Sci 2008, 254, 5886.
26. Sheikh, F.; Barakat, N. A. M.; Chaudhari, A.; Jung, I.; Lee, J.; Kim, H. Macromol Res 2009, 17, 688.
27. Sheikh, F. A.; Barakat, N. A. M.; Kanjwal, M. A.; Jeon, S. H.; Kang, H. S.; Kim, H. Y J Appl Polym Sci 2010, 115, 3189.
28. Demir, M. M.; Yilgor, I.; Yilgor, E.; Erman, B. Polymer 2002, 43, 3303.
29. Pedicini, A.; Farris, R. Polymer 2003, 44, 6857.
30. Baji, A.; Mai, Y. W.; Wong, S. C.; Abtahi, M.; Chen, P. Compos Sci Technol 2010, 70, 703.
31. Xing, S.; Zhao, G. Mater Lett 2007, 61, 2040.
32. Njuguna, J.; Pielichowski, K. J Mater Sci 2004, 39, 3991.
33. Liu, X.; Zhao, Y.; Liu, Z.; Wang, D.; Wu, J.; Xu, D. J Mol Struct 2008, 892, 200.
34. Chen, Z.; Mo, X.; He, H.; Wang, H. Carbohydr Polym 2008, 72, 410.
35. Sahoo, N. G.; Jung, Y. C.; So, H. H.; Cho, J. W. J. Synth Met 2007, 157, 374.
36. Wang, C.; Shieh, Y.; Nutt, S. J Adv Polym Sci 2009, 114, 1025.
37. Katarzyna, M. S.; Gouma, P. J Nanopart Res 2006, 8, 769.
38. Dallas, P.; Niarchos, D.; Vrbanic, D.; Boukos, N.; Pejovnik, S.; Trapalis, C.; Petridis, D. Polymer 2007, 48, 7.
39. Babu, K. F.; Senthilkumar, R.; Noel, M.; Kulandainathan, M. A. Synth Met 2009, 159, 1353.
40. Ciobanu, L. C.; Dorohoi, C. High Perform Polym 2009, 22, 56.
41. Oprea, S. High Perform Polym 2009, 21, 353.
42. Hu, J. L.; Zen, Y. M. Text Res J 2003, 73, 172.
43. Zhang, H.; Chen, Y.; Zhang, Y.; Sun, X.; Ye, H.; Li, W. J Elastomers 2008, 40, 161.
44. Cheng, Q.; He, Y.; Pavlinek, V.; Li, C.; Saha, P. Synthetic Met 2008, 158, 953.
45. Dutta, P.; De, S. K. Synth Met 2003, 139, 201.
46. Saafan, S. A.; El-Nimr, M. K.; El-Ghazzawy, E. H. J Appl Polym Sci 2006, 99, 3370.
47. Barick, A. K.; Tripathy, D. K. Compos A 2010, 41, 1471.
48. El-Meligy, M.; Mohamed, S. H.; Mahani, R. M. Carbohydr Polym 2010, 80, 366.
49. Panwar, V.; Mehra, R. M. Eur Polym J 2008, 44, 2367.
50. Ji, L.; Yao, Y.; Toprakci, O.; Lin, Z.; Liang, Y.; Shi, Q.; Medford, A. J.; Millns, R.; Zhang, X. C. J Power Sources 2010, 195, 2050.